Robotica (2011) volume 29, pp. 733–743. © Cambridge University Press 2010
doi:10.1017/S0263574710000615

Design and operation of a tripod walking robot via dynamics simulation

Conghui Liang*, Hao Gu, Marco Ceccarelli and Giuseppe Carbone

Laboratory of Robotics and Mechatronics, DiMSAT – University of Cassino, Via Di Biasio, 43 – 03043 Cassino (FR), Italy.
E-mails: {hao.gu, ceccarelli, carbone}@unicas.it

(Received in Final Form: September 15, 2010. First published online: October 12, 2010)

SUMMARY
A mechanical design and dynamics walking simulation of a novel tripod walking robot are presented in this paper. The tripod walking robot consists of three 1-degree-of-freedom (DOF) Chebyshev–Pantograph leg mechanisms with linkage architecture. A balancing mechanism is mounted on the body of the tripod walking robot to adjust its center of gravity (COG) during walking for balancing purpose. A statically stable tripod walking gait is performed by synchronizing the motions of the three leg mechanisms and the balancing mechanism. A three-dimensional model has been elaborated in SolidWorks® engineering software environment for a characterization of a feasible mechanical design. Dynamics simulation has been carried out in the MSC.ADAMS® environment with the aim to characterize and to evaluate the dynamic walking performances of the proposed design with low-cost easy-operation features. Simulation results show that the proposed tripod walking robot with proper input torques, gives limited reaction forces at the linkage joints, and a practical feasible walking ability on a flatten ground.

KEYWORDS: Legged walking machines; Tripod walking robots; Leg mechanisms; Dynamics simulation.

1. Introduction

Legged locomotion has a lot of advantages as compared with wheeled and track locomotion when it operates in rough terrain or in unconstructed environment. The potential advantages of legged locomotion can be indicated such as better mobility, obstacles overcoming ability, active suspension, energy efficiency, and achievable speed.[1,2,3,4]

Legged walking robots, such as biped robots, quadrupeds, hexapods, and eight-legged robots, have been studied extensively in the past decades. A lot of prototypes have been built in the laboratories and even for some application tasks.[1,2,3] Significant examples of biped walking robots can be indicated in ASIMO, H7, and HRP, WABIAN series biped humanoid robots, which are capable of imitating some basic human movements, such as dynamic walking, running, descending and ascending stairs, and even jumping.[3,4] Zero moment point (ZMP) theory[5] (ZMP can be defined as the point on the ground about which the sum of all the moments of the active forces equals zero) plays an important role in the dynamic walking control of biped walking robots. Almost all of biped humanoid robots perform dynamic walking by considering the ZMP in the control algorithms.[6,7,8] A quadruped robot, namely, "Bigdog" has been developed in the BostonDynamic Company. The quadruped robot is actuated by using hydraulic actuation system and the robot shows a great walking ability on different rough terrains, such as rock lands, beach, and snow ground, and the robot is even able to walk on the ice surface.[9] Some millstone prototypes in the multilegged walking robots can be considered as the OSU hexapod, PV-II, ASV, TITAN, and ODEX.[1,3] Some recently developed prototypes can be indicated as the quadrupeds Scout I, II[10] in McGill University, six legged RHex[10] of CMU, MARS[11] (Multi Appendage Robotic System) of Virginia Tech, and ATHLETE[12] (All-Terrain Hex-Legged Extra-Terrestrial Explorer), which is the six-legged robotic lunar rover in NASA. These legged robots have on-board actuation, sensor, and control system, and they show outstanding mobility, higher speed, flexibility, and versatility over different irregular terrains. Multilegged walking robots have found several applications such as in military tasks, inspection of nuclear power plants, for movement surveillance, planetary explorations, and for forestry and agricultural tasks.[3,4]

Among legged walking robots, biped walking robots need sophisticate hardware systems and control algorithms to keep its balance during walking. Multilegged robots have a good stable walking performance, and they can operate with several walking gaits. However, the number of motors increases together with legs, and how to coordinate control the motors and gaits synthesis are still difficult problems. Therefore, it is still a challenge issue to develop legged walking robots, which are capable of walking in real environment for tasks, with manipulation and payload transportation capabilities.

At the Laboratory of Robotics and Mechatronics in Cassino, a research line has been devoted to a novel tripod walking robot, which is inspired by some tripod walking in nature, like the old man walking with a cane and kangaroo walking with legs and tail.[13] In ref. [13], a novel biologically inspired tripod walking robot has been proposed with low-cost easy-operation features. A kinematics analysis has been carried out for operation performances evaluation and design purposes. The proposed tripod walking robot can perform a statically stable walking with robust mechanical design and

* Corresponding author. E-mail: liang.conghui@unicas.it

https://doi.org/10.1017/S0263574710000615 Published online by Cambridge University Press

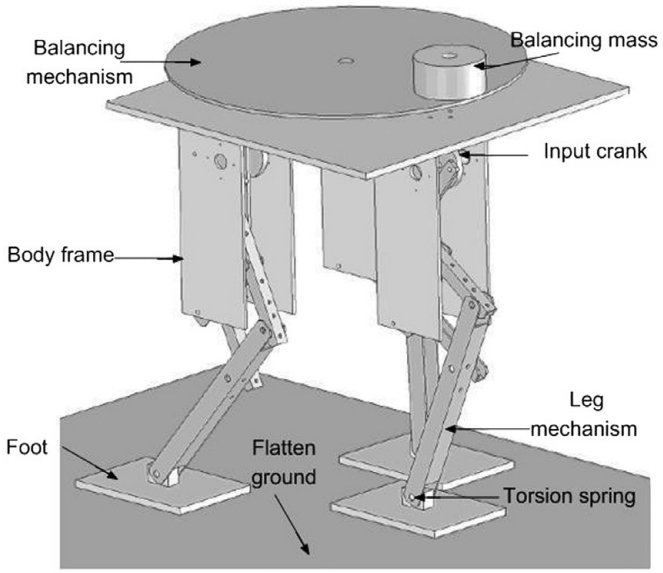


Fig. 1. A 3D model of the proposed tripod walking robot in SolidWorks® environment.

simplified control algorithms. Most of the legged walking robots have even number of legs with symmetrical design configuration. Actually, there are very few works dealing with the tripod walking robots. In refs. [14, 15], STriDER (The Self-Excited Tripedal Dynamic Experimental Robot) is presented as developed at Virginia Tech University. The tripod robot moves by using and controlling the passive dynamic behavior when one leg swings from rear to forth. However, the prototype can only perform one step of walking successfully, and it cannot walk continuously. Another tripod walking robot has been built at the University of Yamagata, Japan.[16] Each leg mechanism of the tripod robot is actuated by two motors, but it is still very difficult to plan and to control its walking gaits.

In this paper, the mechanical design problem of tripod walking robot has been addressed with the aim to build a reliable, robust, and easy-to-control robot, which is capable of moving stably, flexibility, and transportation capability. A three-dimensional (3D) model has been elaborated in SolidWorks® environment with low-cost easy-operation features. Walking stability has been analyzed as linked with the peculiar tripod walking gait. A feasible statically stable tripod walking gait can be performed by synchronizing the motions of the balancing mechanism and the three leg mechanisms. Dynamic walking simulation has been carried out in the MSC.ADAMS® environment to characterize and to evaluate the operation performances of the designed model.

2. The Tripod Walking Robot

A 3D model of the proposed tripod walking robot that has been designed in the SolidWorks® engineering software environment is shown in Fig. 1. The tripod walking robot consists of three 1-degree-of-freedom (DOF) Chebyshev–Pantograph leg mechanisms, a body frame, and a balancing mechanism, which is mounted on the top of body frame. Three leg mechanisms are installed on the body frame in a triangle arrangement with one leg mechanism ahead and two leg mechanisms rear in the same line. The main specifications of the designed model are listed in Table I.

Table I. Main specifications of the 3D model for the tripod walking robot in Fig. 1.

Degrees of freedom	7 (3 of legs, 1 of balancing mechanism, 3 passive at the ankles)
Weight	10 kg
Dimension	300 × 300 × 600 mm
Walking speed	0.36 km/h
Step size	300 mm/step
Walking cycle	1 s/step

The tripod walking robot is developed for payload transportation and manipulation purposes. The proposed design of the tripod walking robot will be capable of moving quickly with flexibility, and versatility within different environments. Therefore, in the mechanical design, particular attentions have been focused to make the tripod walking robot low cost, easy operation, lightweight, and compact. Particularly, commercial products have been extensively used in the designed model to make it easy to build. Aluminum is selected as the material of the tripod walking robot since it has proper stiffness, mass density, and cheap price.

In Fig. 2, a kinematic scheme of a leg mechanism for the tripod walking robot is shown with its design parameters. The 1-DOF leg mechanism is composed of a Chebyshev four-bar linkage LECDB and a pantograph mechanism BGHMIA.

In the Chebyshev four-bar linkage, points L and C are fixed on the body frame. The input variable is the crank rotation angle α, which is defined as the angle between crank LE and horizontal plane. The rocker is link CD and the coupler triangle is EDB. The Chebyshev four-bar linkage can be characterized with the five design parameters m, c, f, d, and a.

While the crank LE rotates around point L, an ovoid coupler curve is traced by point B. The generated ovoid curve is composed of a curve segment and an approximate straight-line segment. During a supporting phase, an approximated straight-line segment is generated for the foot point of the leg mechanism. Therefore, the body of the robot can be propelled efficiently forward with little wave in the vertical direction. The curve segment corresponds to the swinging phase when the leg mechanism swings from rear to forth. One step of walking can be characterized by the step length s and step height h, as indicated in Fig. 2. A detailed kinematics study of the 1-DOF leg mechanism and operation performances evaluation has been carried out for design purpose as reported in refs. [17, 18].

In the pantograph mechanism, point M is fixed on the body frame. The pantograph mechanism can be characterized with the design parameters l_1, l_2, b_1, and b_2. The pantograph mechanism is connected with the Chebyshev linkage at point B. It amplifies the input motion at point B to the output motion at foot point A. The amplify ratio is determined by the length of linkages BH and HA in the pantograph design. The values of the design parameters of leg mechanisms for the 3D model in Fig. 1 are listed in Table II.

https://doi.org/10.1017/S0263574710000615 Published online by Cambridge University Press

Table II. Sizes of design parameters of the leg mechanism in Fig. 2. (in millimeter).

a	*b*	*c*	*d*	*h*	*m*
50	20	62.5	62.5	30	25
f	*p*	l_1	l_2	b_1	b_2
62.5	30	300	200	75	150

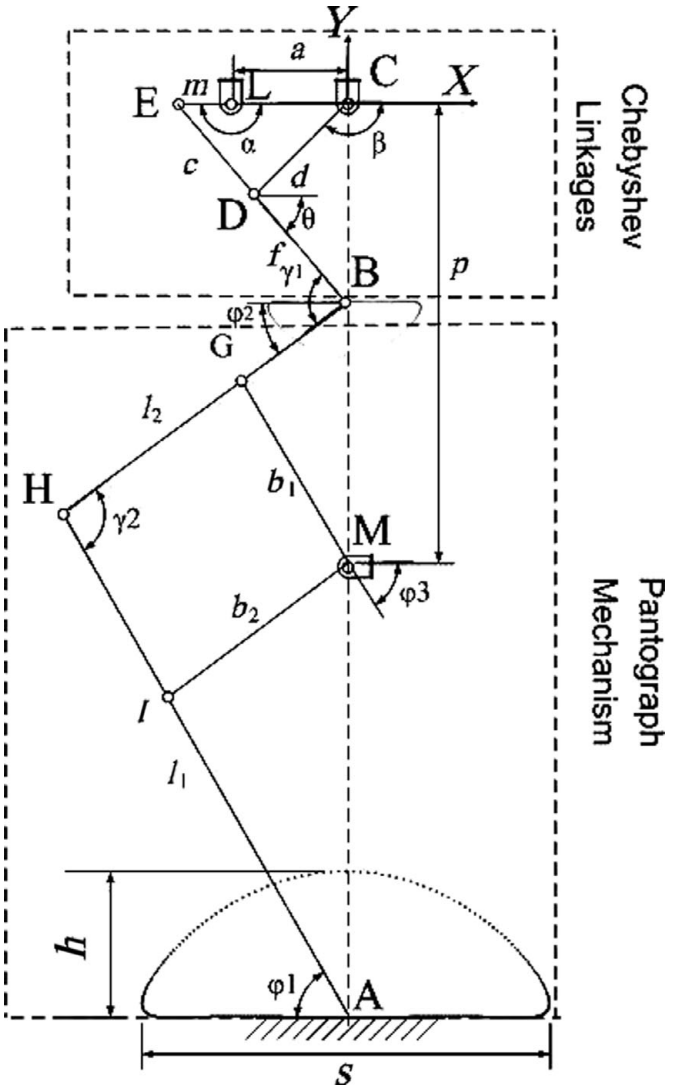


Fig. 2. A kinematic scheme of a leg mechanism with design parameters.

The balancing mechanism is composed of a thin rotation disc and a balancing mass on it as shown in Fig. 3(a). A kinematic scheme with design parameters is shown in Fig. 3(b), where the parameter m_b is the mass of the balancing mass, r is the distance between the center of the disc and the balancing mass, and ψ is its rotation angle. The sizes of the design parameters can be determined so that the tripod walking robot can perform a statically stable walking gait. A plane foot is connected at the end of each leg mechanism by using a passive torsion spring. The torsion spring makes the foot in contact with the ground with a suitable compliance. Therefore, the tripod walking can walk stable, even for rough terrains.

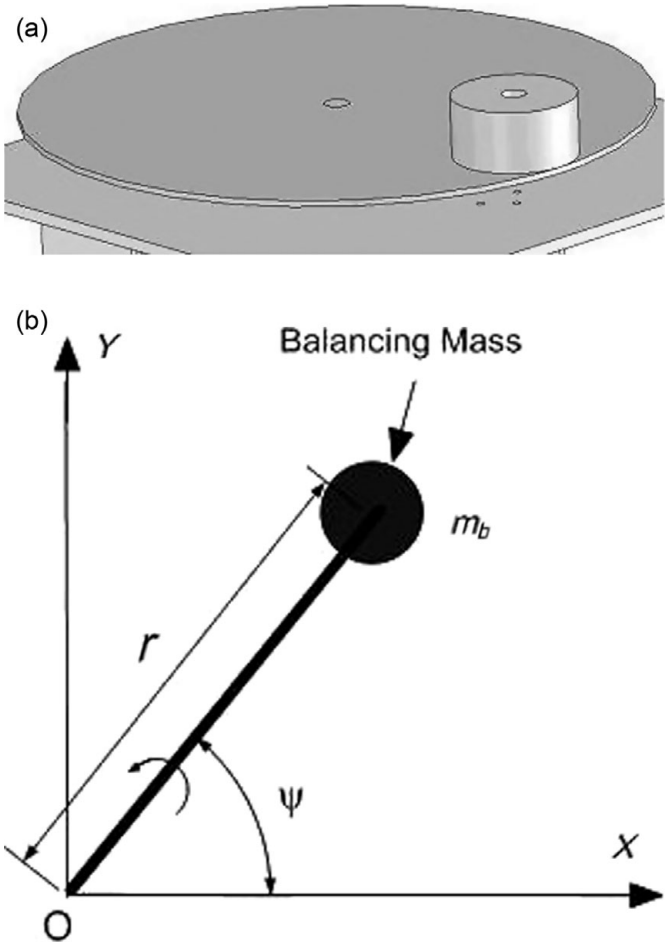


Fig. 3. The balancing mechanism; (a) a 3D model; (b) a kinematic scheme with design parameters.

In a standing phase, the COG projection on the horizontal plane of the tripod walking robot falls within the triangle, which is determined by three legs in contact with the ground. In this condition, a very good static balance can be obtained and the tripod walking robot can implement tasks with a manipulator that is installed on its body. In the motion phase, there are always two legs in contact with the ground at the same time and propelling the body forward, while the third leg swings from rear to forth. By adjusting the COG projection point of the robot in the support polygon, the static equilibrium can be achieved easily. The convex polygon can be identified as formed by connecting footprints of the robot on the ground. Therefore, the robot can be used for transportation purposes since it walks in static equilibrium.

3. A Characterization of the Tripod Walking Gait

Figure 4 shows a scheme of the feet configuration in the horizontal plane with its design parameters. A_1 and A_2 represent the supporting feet, which are in contact with the ground, and A_3 represents the swinging foot in the air. The COG projection point on the horizontal plane of the tripod walking robot is indicated as a circle. The support polygon that is formed by using the supporting feet areas, is indicated with gray color as characterized by f_1, f_4, f_5, and f_6. The

https://doi.org/10.1017/S0263574710000615 Published online by Cambridge University Press

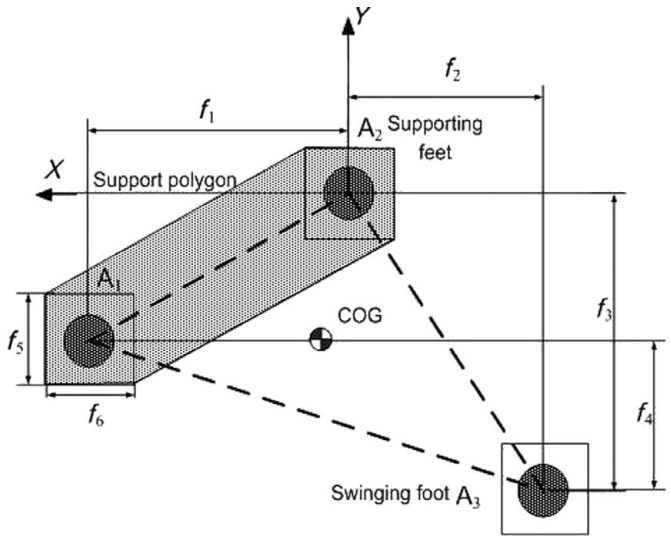


Fig. 4. A scheme of the feet projection with COG in the horizontal plane with design parameters.

size of a foot can be indicated by f_5 and f_6, as shown in Fig. 4.

An operation performance analysis of the proposed tripod walking robot has been carried out in MATLAB® with properly formulated kinematics equations as reported in ref. [13].

A numerical result for the computed tripod walking gait is shown in Fig. 5 for the characterization and design purposes. The tripod walking robot is shown in the saggital plane and horizontal plane for three different walking phases, which correspond to different leg mechanisms in the swinging phase. In phase I, the feet A_1 and A_2 are in contact with the ground while the A_3 foot swings in the air. In phase II and phase III, feet A_1 and A_2 perform the swinging motion in the air, respectively. The corresponding input crank angles of α_1 for different walking phases are also indicated.

A diagram is shown in Fig. 6 for the tripod walking gait with its parameters. The tripod walking gait is a kind of 3-1-2 walking gait, as shown in Fig. 6(a). The tripod gait starts at t_0, when foot A_3 leaves the ground, while A_1 and A_2 feet are in contact with the ground at the same time. The convex hull of the contact points and the COG projection of the robot are plotted in Fig. 5(a). When feet A_3 touches on the ground at time t_1, foot A_1 leaves the ground with feet A_2 and A_3 are the supporting feet, as shown in Fig. 5(b). The third walking phase is performed with foot A_2 moving in the air at time t_2 to t_3, and a full cycle of tripod walking gait is completed going back to a starting configuration for a new gait cycle. The simulated walking gait is characterized by the supporting time T_g and swinging time T_a, as shown in Fig. 6(b). The time of a full cycle of tripod walking gait is computed as $T = T_g + T_a$ with $T_g = 2 \times T_a$, where T_g is the time period that the foot is in contact with the ground and T_a is the time period that a leg swings in the air.

As shown in Fig. 5, although there are always two feet in contact with the ground, the COG projection of the tripod walking robot does not fall inside the convex hull, and therefore, the tripod walking robot cannot perform stable walking with static equilibrium. By increasing the

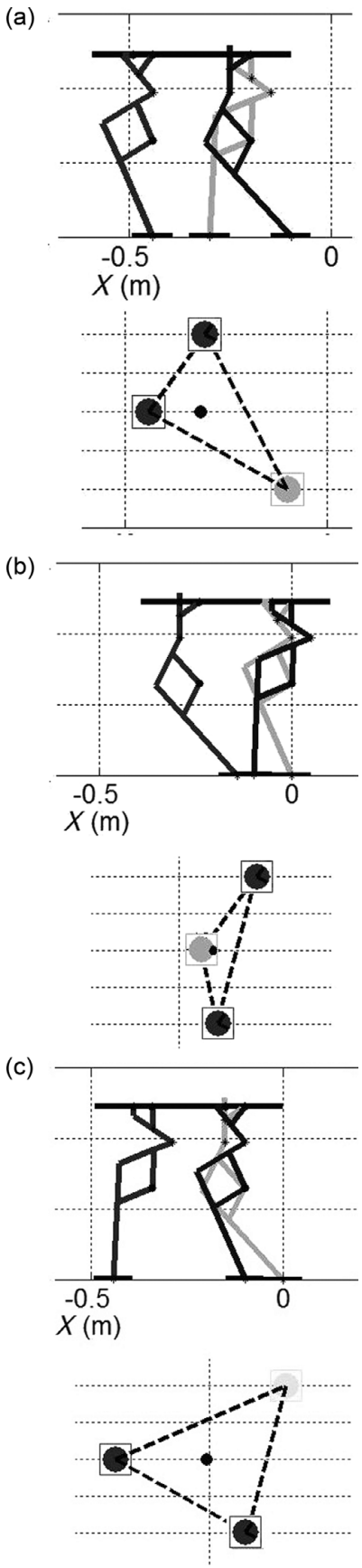


Fig. 5. A computed sequence of the tripod walking gait in saggital and horizontal plane; (a) phase I: $\alpha_1 = 180^\circ$ with feet A_1 and A_2 are on the ground; (b) phase II: $\alpha_1 = 270^\circ$ with feet A_2 and A_3 are on the ground; (c) phase III: $\alpha_1 = 90^\circ$ with feet A_1 and A_3 are on the ground.

https://doi.org/10.1017/S0263574710000615 Published online by Cambridge University Press

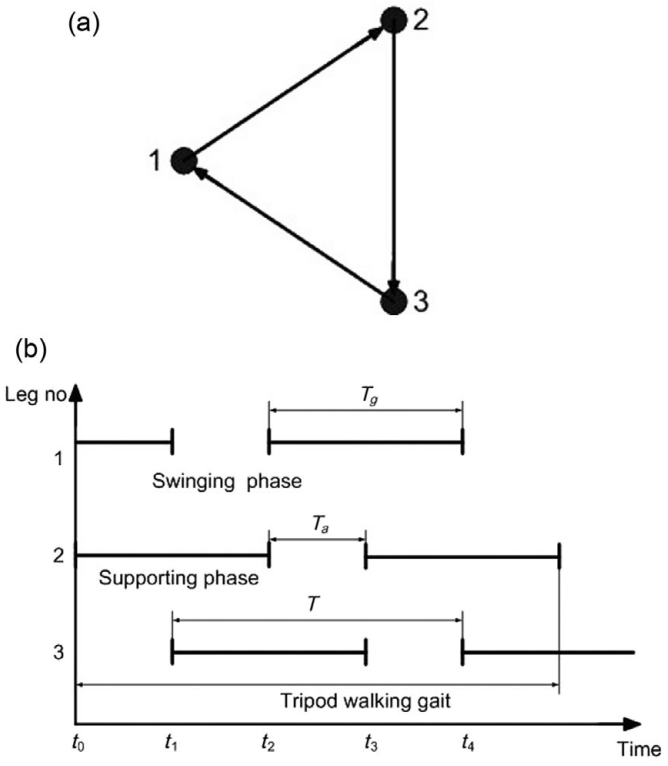


Fig. 6. Walking gaits of the tripod walking robot; (a) a 3-1-2 gait; (b) a gait diagram.

dimensions of the foot areas (parameters f_5 and f_6), the support polygon can be large enough to fulfill the statically walking condition. However, it is not feasible to anticipate that a tripod walking robot can move efficiently and has a good adaptability with different terrains with big and heavy feet. Therefore, the COG projection of the robot is needed to be adjusted during the walking cycle so that a statically equilibrium can be ensured with proper foot size. The balancing mass, which is installed on the body frame, can be used for COG position adjustment purpose.

4. A Stability Analysis with a Balancing Mass

Walking stability is an important issue for legged walking robots, since they have only discrete contact points between the legs and the ground. Therefore, it is easy for them to tip over and fall down especially when it walks on a rough terrain.

Actually, there are two modes of walking for legged walking robots from stability viewpoint, namely, statically stable walking and dynamically stable walking.[2] The dynamically stable walking can be achieved by controlling the position of ZMP of the robot to be inside the support polygon so that the robot can walk stably without unbalance configuration. Similarly, the statically stable walking can remain statically stable if-and-only-if its COG projects vertically inside the support polygon.[3]

Figure 7 is a scheme of the feet projection on the horizontal plane with the balancing mass for the COG adjustment purpose. The stability margin S_m is defined as the distance of the vertical projection of COG from the boundaries of the support polygon in the horizontal plane. By selecting proper parameters for the length of rotation bar r and the weight of balancing mass m_b, the COG projection point of

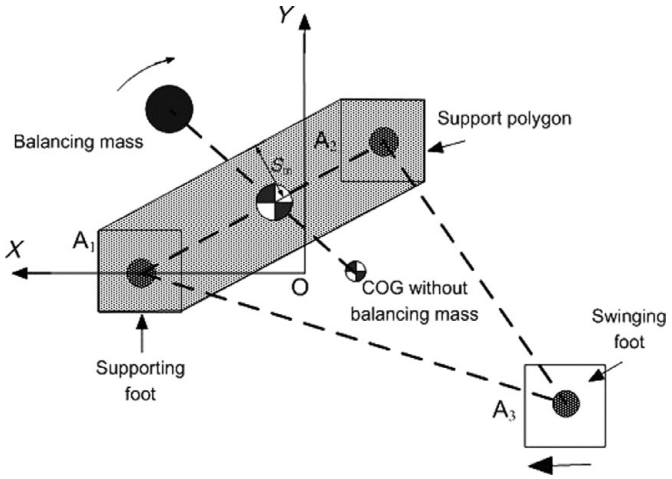


Fig. 7. A scheme for balancing mass motion in adjusting the COG projection during walking.

the robot can be adjusted inside the support polygon for different walking phases, by synchronizing the motion of the balancing mass with the operation of leg mechanisms. Thus, the tripod walking robot can perform a static stability walking even on a rough terrain.

For the tripod walking robot, since the mass center of each link is in its geometry center, the mass center coordinates for each leg mechanism can be computed by using the expression

$$x_{mi} = \frac{\sum_{j=1}^{7} m_{ij} x_{ij}}{\sum_{j=1}^{7} m_{ij}}, \qquad y_{mi} = \frac{\sum_{j=1}^{7} m_{ij} y_{ij}}{\sum_{j=1}^{7} m_{ij}}, \tag{1}$$

where x_{ij} and y_{ij} $(i = 1, \ldots, 3), (j = 1, \ldots, 7)$ are the coordinates of the mass center of each link for the ith leg mechanism, m_{ij} is the mass of the jth link, x_{mi} and $y_{mi} (i = 1, 2, 3)$ are the coordinates of mass center of the ith leg mechanism. By using the scheme in Fig. 3(b), the coordinates of the balancing mass can be computed as

$$x_b = r \cos \psi, \quad y_b = r \sin \psi. \tag{2}$$

Therefore, by using Eqs. (1) and (2), the coordinates x and y of the mass center of the whole robot can be computed as

$$\left.\begin{aligned} x &= \frac{\sum_{i}^{3} m_i x_{mi} + x_b m_b + x_r m_r}{\sum_{i}^{3} m_i + m_b + m_r}, \\ y &= \frac{\sum_{i}^{3} m_i y_{mi} + y_b m_b + y_r m_r}{\sum_{i}^{3} m_i + m_b + m_r}, \end{aligned}\right\} \tag{3}$$

where m_r is the mass of the body frame and m_b is the mass of the balancing mass.

As pointed out in ref. [13], the rotation velocity of input crank in a leg in the swinging phase is twice than that at the leg in supporting phase. Considering that the rotation velocity of the input crank is ω rad/s, when the leg is in contact with the ground, the rotation velocity is 2ω rad/s, when the leg swings

https://doi.org/10.1017/S0263574710000615 Published online by Cambridge University Press

in the air. Therefore, the rotation angle of the balancing mass should be $2\pi/3$, while a leg mechanism finishes a swinging phase at an angle of π. Thus, the input rotation velocity for the balancing mass can be computed as

$$\omega_b = 2\omega \frac{\pi}{(2\pi/3)} = 3\omega. \quad (4)$$

In order to make the robot compact, the rotation bar is designed not to exceed the dimension of the body frame, and the balancing mass will be not too heavy for energy efficient purpose. Figure 8 shows the feet projections for three different walking phases after COG position adjustments as referring to the curves in Fig. 8. The locus of the COG projection point is plotted with bold lines. It can be noted that the projection of the COG in horizontal plane is always inside the support polygon and the stability margin is $S_m > 0$. In this condition, the tripod walking robot is able to perform a statically stable walking on a flatten ground. Particularly, at the transition period of different walking phases, the stability margin S_m becomes smaller. However, the tripod walking robot is in a tripod supporting phase,[12] which is the short period of time designing, which all the three legs are in contact with the ground. Thus, the robot still has a good stability for walking operation.

5. Dynamics Walking Simulation

A 3D model that has been elaborated in SolidWorks® environment is shown in Fig. 1, and then it has been imported to MSC.ADAMS® environment with suitable further modeling, as shown in Fig. 9. 3D solid contacting constraints have been added for simulating the contact behavior between the feet and the ground. Friction has been prescribed for ground contact by using a coulomb friction model in the simulation environment.

The reference system for the measured characterization values is fixed on the ground in the MSC.ADAMS simulation environment, which is a world frame, as shown in Fig. 9. The input torques for the leg mechanisms and the balancing mass are indicated, as shown in Fig. 9 as τ_1, τ_2, τ_3, and τ_b. The reaction force at the knee points and between the feet and ground are indicated as f_1, f_2, f_3 and F_1, F_2, F_3, respectively. These characteristics are useful to evaluate the proposed tripod design for a practical feasible operation and optimal design purposes. In the simulation, the mass center is set in the geometry center of each element. The mass value of each component are listed in Table III as m_{LE}, m_{EB}, m_{CD}, m_{BI}, m_{PH}, m_{HA}, m_{BG}, m_f for a leg mechanism, and m_r and m_b are the mass of the body frame and balancing mass, respectively. Simulation time has been prescribed in 3 s to simulate a full cycle of tripod walking gait, during which 500 simulation steps are computed. The friction coefficient between the feet and the ground has been set equal to 0.9.

The input motions for the three leg mechanisms and the balancing mass are prescribed by using the STEP function in the MSC.ADAMS® environment. Figure 10 shows the input angular velocities as function of time at the cranks of three leg mechanisms. The angular velocity for the balancing

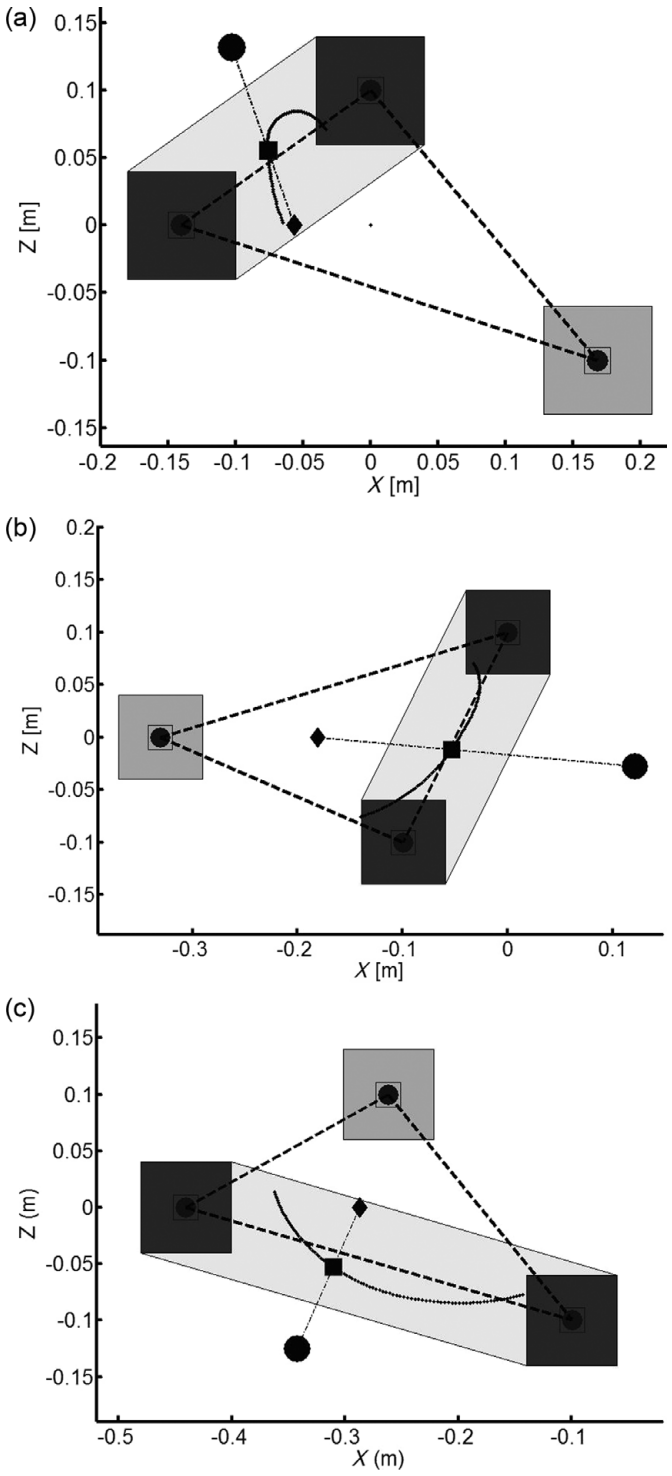


Fig. 8. A tripod walking gait with the locus of COG and support polygon with balancing mass for the cases in Fig. 5; (a) walking phase I; (b) walking phase II; (c) walking phase III.

mechanism has been set as $2\pi/3$ rad/s as synchronized with the motion of leg mechanisms.

As shown in Fig. 10, the input angular velocity has been set as $\pi/2$ rad/s, when the leg is in the supporting phase, as π rad/s, when the leg is in the swinging phase. Particularly, since leg 3 is installed on the opposite side with respect to legs 1 and 2, thus the input angular velocity is positive. The angular velocities at the transition points have been smoothed

https://doi.org/10.1017/S0263574710000615 Published online by Cambridge University Press

Table III. The mass of components for the simulated model in Fig. 9 (in kilogram).

m_{LE}	m_{EB}	m_{CD}	m_f	m_r
0.025	0.05	0.025	0.2	1
m_{BI}	m_{PH}	m_{HA}	m_{BG}	m_b
0.035	0.08	0.11	0.025	2

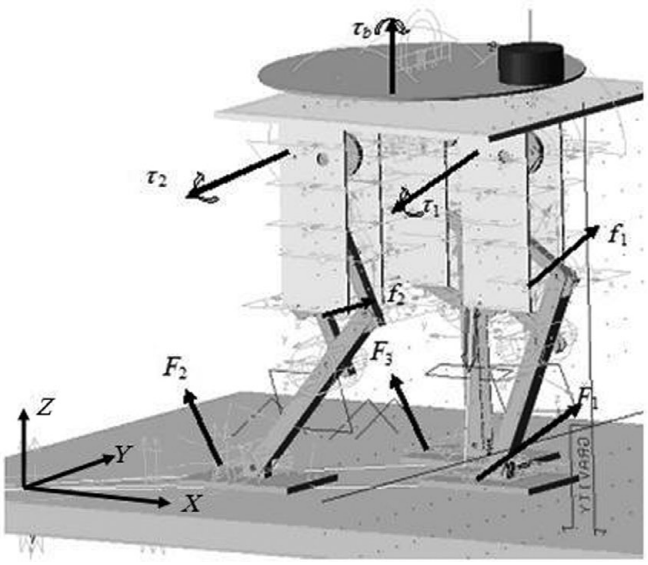


Fig. 9. A 3D model of the tripod walking robot in the MSC.ADAMS® environment for dynamics walking evaluation.

by using spine curves so that a practical feasible solution can be obtained.

6. Simulation Results

By using the corresponding functions that are available in the MSC.ADAMS® environment, the input torques for actuation motors, reaction forces at link joints of the leg mechanisms, as well as the displacements and walking speed of the tripod walking robot are obtained. These results are useful performance indexes for evaluating a practical feasible design solution for the tripod walking robot.

The computed input actuation torques at the crank of three leg mechanisms are reported in Fig. 11. The torque curves for three leg mechanisms are indicated as solid, dot-dashed, and dashed lines, respectively. These torque curves are useful for selecting actuators with proper sizes and output power.

The torque curves are similar with each other with only a period of time delay. The peak value has been computed as less than 3 N mm. At 0.1, 1.2, and 2.1 s, there is a jump in the torque, which is caused by the corresponding leg that lands on the ground. Particularly, the impact torque at 2.1 s is much lager than the other two, because at this time the first leg lands on the ground while the balancing mass is just on the top of this leg mechanism. Displacements of the foot points A_1, A_2, and A_3 along X-axis and Y-axis are shown in Fig. 12(a).

From the simulation, the robot moves the third leg (A_3) first with a step length of 300 mm. Then, the first leg (A_1) is moved and finally the second leg (A_2). Therefore, a 3-1-2

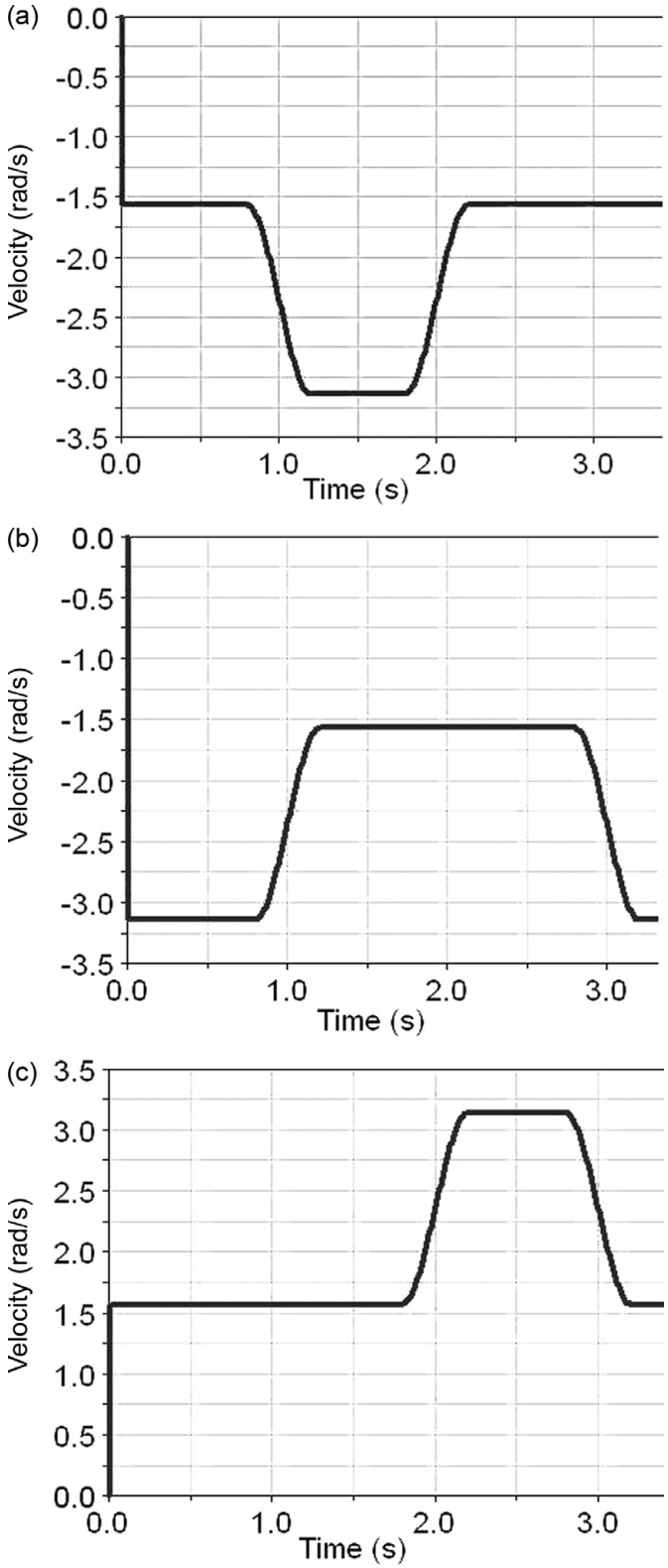


Fig. 10. Input angular velocities for three leg mechanisms; (a) for leg 1; (b) for leg 2; (c) for leg 3.

tripod walking gait has been achieved, as shown in Fig. 6(b). The corresponding displacements of the foot points along Y-axis are shown in Fig. 12(b), and the step height H can be computed as about 40 mm for each step.

For legged walking robots, the contact forces between the feet and the ground should be maintained with proper values.

https://doi.org/10.1017/S0263574710000615 Published online by Cambridge University Press

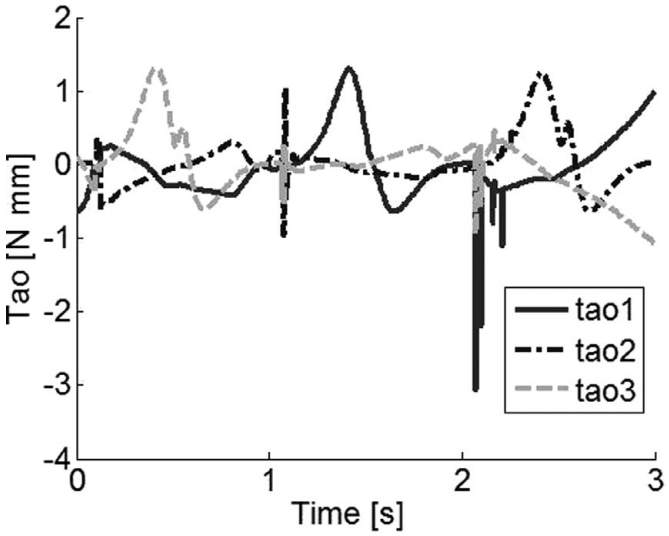


Fig. 11. Computed actuation torques $\tau_i (i = 1, 2, 3)$ at the crank for three leg mechanisms.

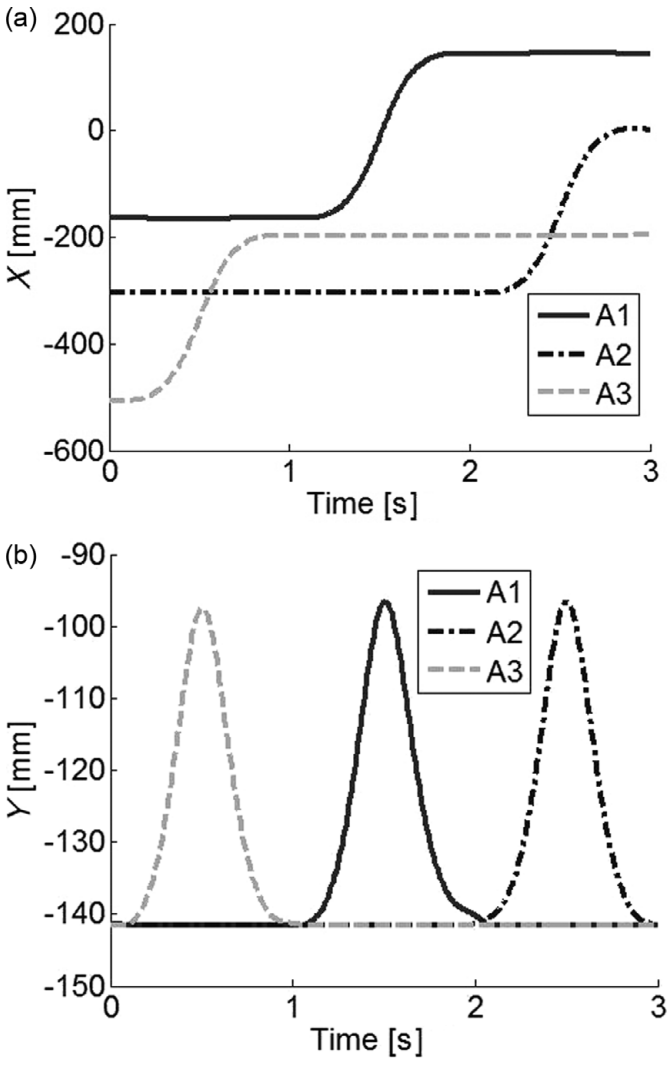


Fig. 12. Computed displacements of foot points $A_i (i = 1, 2, 3)$ with respect to time; (a) along X-axis; (b) along Y-axis.

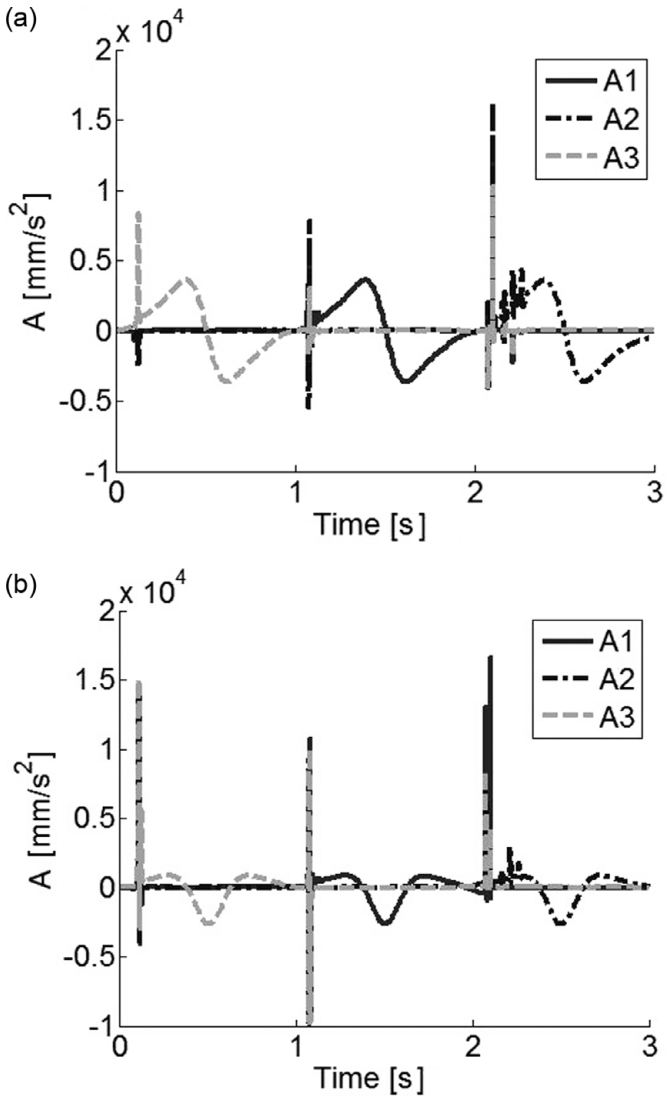


Fig. 13. Computed accelerations of the feet points $A_i (i = 1, 2, 3)$ for three leg mechanisms; (a) along X-axis; (b) along Y-axis.

Otherwise, too large contact forces will greatly deteriorate the walking stability of the robot and even damage the mechanical structure of the robot. Figures 13(a) and (b) show the accelerations of the foot points $A_i (i = 1, 2, 3)$ along X-axis and Y-axis, respectively. At 0.1, 1.1, and 2.1 s, there are three peak values when the corresponding leg lands on the ground. The maximum peak value has been computed as 20m/s^2, and then the acceleration is decreased quickly. This peak acceleration can be considered not a large value since the strike acceleration in human steel during a normal walking is generally large than 50m/s^2.[19]

The displacements of the COG for the tripod walking robot along X-axis and Y-axis are plotted in Figs. 14(a) and (b), respectively. The tripod walking robot moves 300 mm along X-axis in a straight line during a full tripod walking gait. The average walking speed has been computed as 100 mm/s according to V_X in Fig. 14(b). The motion velocity is not constant since the leg mechanisms propelling the body move with a nonconstant speed in the supporting phases as reported also in ref. [13].

https://doi.org/10.1017/S0263574710000615 Published online by Cambridge University Press

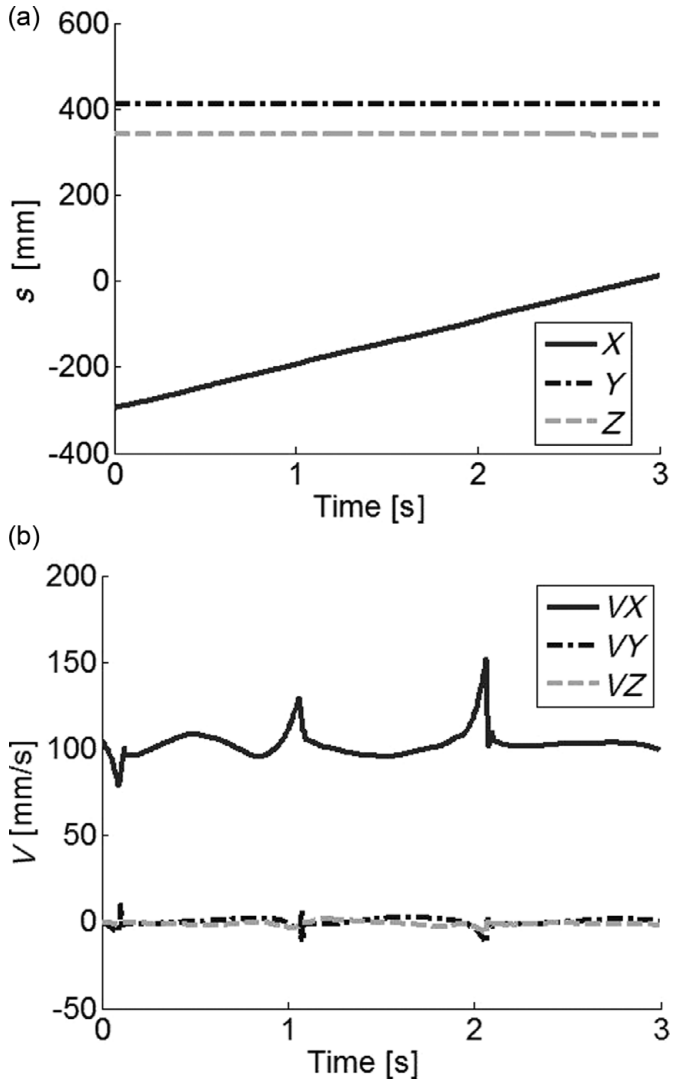


Fig. 14. Computed position and velocity of COG for the tripod walking robot; (a) displacement components; (b) velocity components.

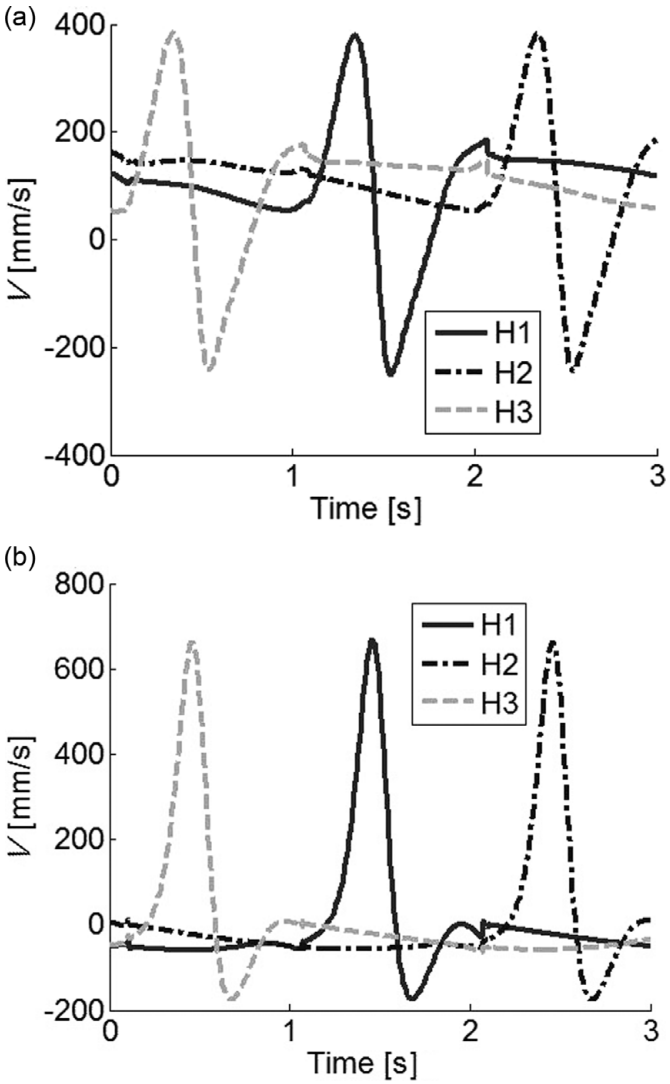


Fig. 15. Displacement velocities of the kneel points $H_i (i = 1, 2, 3)$ with respect to time; (a) along X-axis; (b) along Y-axis.

The reaction forces at link joints are useful to evaluate the motion transmission efficiency within the mechanisms. A too large reaction force requires unfeasible input actuation torque, and it is possible to break the mechanical structure of the robot. The displacement velocities at the knee points $H_i (i = 1, 2, 3)$ along X-axis and Y-axis are plotted in Figs. 15(a) and (b), respectively. The maximum velocity along X-axis has been computed as 400 mm/s, and it is twice times than the velocities of foot points. The velocity along Y-axis has been computed as 600 mm/s, and it is a feasible value.

In Fig. 16, snapshots of the walking sequences during simulation are shown. Corresponding simulation time is indicated for each snapshot. We can see that the designed model of the tripod walking robot walks on the ground with a desired 3-1-2 tripod walking gait. The motion of the balancing mass are synchronized with the motion of the leg mechanisms to keep the tripod walking robot walking stable.

7. Conclusions

A mechanical design and dynamics walking simulation have been presented for a new tripod walking robot in this paper. A 3D model has been elaborated in the SolidWorks® engineering software environment for the evaluation design performances and checking the operation feasibility. The designed model inherits several advantages, such as low cost, easy operation, compactness, and lightweight so that the proposed tripod walking robot can move efficiently in a real environment. Statically walking can be performed by properly operating a balancing mass and synchronizing the motion of leg mechanisms, as shown from the reported simulation results. Dynamics walking simulation of the designed model has been carried out in the MSC.ADAM® environment. Simulation results show that the proposed mechanical designed model with proper input torques for the actuation motor can give suitable limited reaction forces at linkage joints and a stable walking ability on the flat ground.

Acknowledgments

C. Liang and H. Gu would like to acknowledge the Chinese Scholarship Council (CSC) for supporting their Ph.D. study and research at the Laboratory of Robotics and

https://doi.org/10.1017/S0263574710000615 Published online by Cambridge University Press

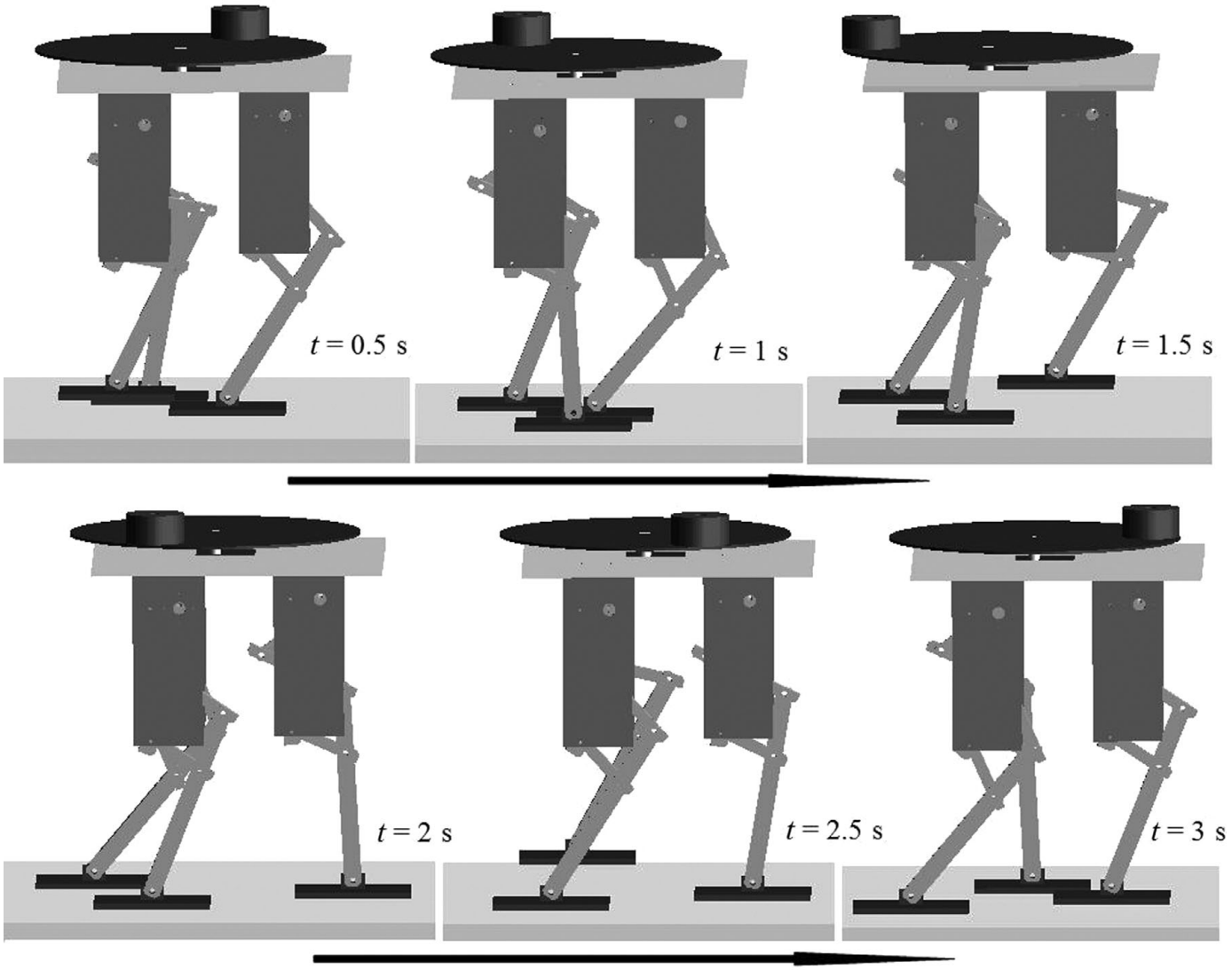


Fig. 16. Snapshots of the simulated walking sequence of the tripod walking robot in the MSC.ADAMS® dynamics simulation environment.

Mechatronics (LARM) in the University of Cassino, Italy, for 2008–2010.

References

1. S. M. Song and K. J. Waldron, *Machines That Walk-The Adaptive Suspension Vehicle* (The MIT press, Cambridge, 1989).
2. P. González-de-Santos, E. Garcia and J. Estremera, *Quadrupedal Locomotion: An Introduction to the Control of Four-legged Robots* (Springer-Verlag, New York, 2006).
3. G. Carbone and M. Ceccarelli, "Legged Robotic Systems," *Cutting Edge Robotics ARS Scientific Book* (Springer-Verlag, Wien, 2005) pp. 553–576.
4. B. Siciliano and O. Khatib, *Springer Handbook of robotics, Part G, legged robots* (Springer-Verlag, Berlin Heidelberg, 2008).
5. M. Vukobratovic, B. Borova, D. Surla and D. Storic, *Biped Locomotion: Dynamic Stability, Control and Application* (Springer-Verlag, New York, 1989).
6. S. Kajita, F. Kanehiro, K. Kaneko, K. Fujiwara, K. Harada, K. Yokoi and H. Hirukawa, "Biped walking pattern generation by using preview control of zero-moment point," *Int. Conf. Robot. Autom.* Taiwan, **1**, 1620–1626 (2003).
7. T. Sugihara, Y. Nakamura and H. Inoue, "Realtime humanoid motion generation through ZMP manipulation based on inverted pendulum control," *Int. Conf. Robot. Autom.* Washington, DC, **1**, 1404–1409 (2002).
8. Q. Huang, K. Yokoi, S. Kajita, K. Kaneko, H. Arai, N. Koyachi and K. Tanie. "Planning walking patterns for a biped robot," *IEEE Trans. Robot. Autom.* **17**(3), 280–289 (2001).
9. M. Raibert, "BigDog, the Rough-Terrain Robot," *17th IFAC World Congress, Plenary Talk*, (2008).
10. M. Buehler, "Dynamic locomotion with one, four and six-legged robots," *J. Robot. Soc. Japan* **20**(3), 15–20 (2002).
11. W. H. Dennis, "Biologically inspired locomotion strategies: novel ground mobile robots at RoMeLa," *3rd Int. Conf. Ubiquitous Robot. Ambient Intelligence.* **1**, 23–28 (2006).
12. B. H. Wilcox, T. Litwin, J. Biesiadecki, J. Matthews, M. Heverly, J. Morrison, J. Townsend, N. Ahmad, A. Sirota and B. Cooper, "Athlete: A cargo handling and manipulation robot for the moon," *J. Field Robot.* **24**(5), 421–434 (2007).
13. C. Liang, M. Ceccarelli and G. Carbone, "A novel biologically inspired tripod walking robot," *13th WSEAS Int. Conf. Computers.* Rodos Island, **60** (141), 83–91 (2009).
14. J. R. Heaston, *Master's thesis: Design of a Novel Tripedal Locomotion Robot and Simulation of a Dynamic Gait for a Single Step* (VA: Polytechnic Institute and State University, Blacksburg, 2006).

https://doi.org/10.1017/S0263574710000615 Published online by Cambridge University Press

15. D. Kamerling and P. Larochelle, "Proposed design of a triped robot," *Florida Conf. Rec. Adv. Robot.* Florida, **1**, 253–258 (2007).
16. I. Hiromasa, F. Kazuhiro, O. Naomichi and M. Kazuhisa, "Mechanism and control of a tripedal walking robot," *Nippon Robotto Gakkai Gakujutsu Koenkai Yokoshu* **18**, 215–216, (2000).
17. E. Ottaviano, M. Ceccarelli and C. Tavolieri, "Kinematic and Dynamic Analyses of a Pantograph-Leg for a Biped Walking Machine", *In CD Proceedings of the 7th International Conference on Climbing and Walking Robots (CLAWAR 2004)*, Madrid, Spain (2004), Paper: A019.
18. C. Liang, M. Ceccarelli and Y. Takeda, "Operation Analysis of a One-DOF Pantograph Leg Mechanism", *In CD Proceedings of the 17th International Workshop on Robotics in Alpe-Adria-Danube Region*, Ancona (2008), Paper: 50.
19. J. Rose and J. Gamble, *Human Walking – the 3rd Edition* (Lippincott Williams & Wilkins, 2005).

https://doi.org/10.1017/S0263574710000615 Published online by Cambridge University Press